#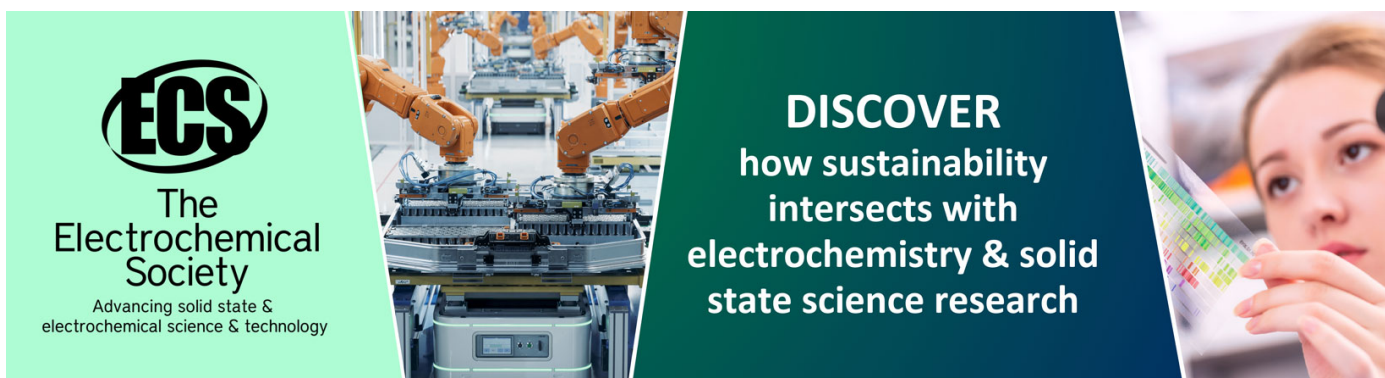 Low percolation transitions in carbon nanotube networks dispersed in a polymer matrix: dielectric properties, simulations and experiments

View the article online for updates and enhancements.

You may also like

Low percolation transitions in carbon nanotube networks dispersed in a polymer matrix: dielectric properties, simulations and experiments

Ricardo Simoes[1,2], **Jaime Silva**[1,3], **Richard Vaia**[4], **Vítor Sencadas**[3], **Pedro Costa**[3], **João Gomes**[3,5] and **Senentxu Lanceros-Méndez**[3]

[1] IPC—Institute for Polymers and Composites, University of Minho, Campus de Azurem, 4800-058 Guimaraes, Portugal
[2] School of Technology, Polytechnic Institute of Cavado and Ave, 4750 Barcelos, Portugal
[3] Department of Physics, University of Minho, Campus de Gualtar, 4710-057 Braga, Portugal
[4] Air Force Research Laboratories, Wright-Patterson AFB, OH 45433-7750, USA
[5] CeNTI—Centre for Nanotechnology and Smart Materials, Rua Fernando Mesquita, 2782, 4760-034 Vila Nova de Famalicao, Portugal

E-mail: rsimoes@dep.uminho.pt, rsimoes@ipca.pt and lanceros@fisica.uminho.pt

Abstract

The low concentration behaviour and the increase of the dielectric constant in carbon nanotubes/polymer nanocomposites near the percolation threshold are still not well understood. In this work, a numerical model has been developed which focuses on the effect of the inclusion of conductive fillers in a dielectric polymer matrix on the dielectric constant and the dielectric strength. Experiments have been carried out in carbon nanotubes/poly(vinylidene fluoride) nanocomposites in order to compare to the simulation results. This work shows how the critical concentration is related to the formation of capacitor networks and that these networks give rise to high variations in the electrical properties of the composites. Based on numerical studies, the dependence of the percolation transition on the preparation of the nanocomposite is discussed. Finally, based on numerical and experimental results, both ours and from other authors, the causes of anomalous percolation behaviour of the dielectric constant are identified.

(Some figures in this article are in colour only in the electronic version)

1. Introduction

The study of the dielectric constants of composites containing conductive or insulating materials has been an intense research area in past decades [1]. Particularly interesting are carbon nanotube/polymer nanocomposites due to their application potential. In these particular composites, the nanotube concentration, aspect ratio, and dispersion significantly affect the material response [2].

Models have been developed that can predict, to some extent, the effect on the permittivity of adding conductive fillers to a lossless dielectric matrix [3, 4]. The effective mean-field medium concept is the foundation for most of the empirical models. The main drawback of these models is that they fail to predict the composite dielectric behaviour near the percolation threshold, defined as the critical point where the physical properties have singularities and show scaling behaviour [5, 6].

There are some experimental results in composites prepared by the addition of Multiwall carbon nanotubes MWCNT to a polymeric matrix. Wang and Dang [7] reported a low concentration (0.0161) for the percolation point of MWCNT/poly(vinylidene fluoride) (PVDF), Ahmad and Pan [8] also reported a low concentration (0.0079)

for alumina/MWCNT, and Zhu *et al* [9] reported for MWCNT/polyimide composites, a concentration of (0.07). The later concentrations represent the fillers volume fraction.

For interpretation of the obtained values, Zhu [9] related the lower values of the concentration necessary to achieve the percolation threshold with the high aspect ratio of the MWCNT, and the increase of the dielectric constant with the formation of conductive paths. Wang and Dang [7], as well as Ahmad and Pan [8], associate the lower concentrations also with the fillers' high aspect ratio and the increase of the dielectric constant with formation of mini-capacitor networks when the concentration increases.

Munson-McGee [10] developed a formulation based on statistical arguments for estimating the critical volume fraction of cylinders for the formation of 3D percolative networks. Depending on the aspect ratio and orientation, the critical volume fraction varied from less than 0.01 to greater than 0.20. For instance, the critical concentration for the formation of a percolative network with a 3D random distribution of cylinders with an aspect ratio of 500 is ~0.01. If we compare the reported experimental values (0.0161, 0.0079, 0.07) with the theoretical ones, a divergence is found. This can be taken as an indication that physical contact does not explain the percolation threshold, despite the fact that (0.0161) is of the same order of magnitude of the theoretical values for an aspect ratio of 500.

It can be thus concluded that the increase of the dielectric constant near the percolation threshold is not yet well understood. This problem is addressed in the present work by developing a numerical model and comparing it to experimental results, focusing on the effect of incorporating nanotubes in the nanocomposite on the dielectric constant and dielectric strength.

2. Experimental procedure

A commercial Solef 1010 poly(vinylidene fluoride) (PVDF) was supplied by *Solvay, Inc.* (Belgium) and a high purity multiwalled carbon nanotube (Baytubes C 150P, MWCNT; purity > 95%, outer mean diameter = 13–16 nm length = 1–10 μm) was supplied from Bayer materials science.

Pristine MWCNT were placed inside an Erlenmeyer with 50 ml of toluene kept inside an ultrasound bath (*Bandelin*, Model Sonorex Super RK106) during 6 h to promote a good dispersion of the MWCNT in the suspension. Afterwards, the solution was kept inside an oven (*Selecta*, Model 2000208) at 120 °C for 24 h to dry the MWCNT. In the next step, an electric discharge of 20 kV was applied for 30 min to the MWCNT by a *home-made* Corona setup apparatus. This procedure helps to disperse and reduce the aspect ratio of the MWCNT.

At the end of the electric discharge, the MWCNT was placed inside an Erlenmeyer with N, N-dimethyl formamide (DMF pure grade, from *Merck*) in a ratio of 1 g of PVDF for 4 ml of DMF. This solution was once again stirred in the ultrasound bath for 3 h. After this time, the desired amount of PVDF was added to the solution and again stirred for a complete dissolution of the polymer.

Flexible films were obtained by spreading the solution on a clean glass substrate. Solvent evaporation and polymer crystallization were obtained inside an oven (*Selecta*, model 2000208) at a controlled temperature. The samples were maintained inside the oven for 60 min at 120 °C to ensure the complete crystallization of the nanocomposite and complete removal of the solvent. After the crystallization process, samples were melted at 230 °C for 15 min and cooled down to room temperature. This procedure produced α-phase samples. The volume fraction of MWCNT varied from 7.8×10^{-6} to 3.89×10^{-3}.

Dielectric measurements were performed using a Quadtech 1920 LCR precision meter at room temperature in the 20 Hz–1 MHz frequency range. Previously, ~5 mm diameter Al electrodes were deposited by thermal evaporation on the ~20 μm samples.

Dielectric breakdown curves were obtained at room temperature using a Radiant Ferroelectric Premier II LC to obtain $I–V$ and $I–E$ curves in real-time. Each sample was submitted to increasing applied voltages until the final breakdown of the material, and the breakdown voltage was obtained by determining the special points of I versus V where the current begins to rise from the initial low current values [11].

3. Theoretical background

The inclusion of carbon conductive fillers in a dielectric matrix enhances composite electrical properties. The most remarkable aspect of these composites is that after the percolation threshold—the critical point where physical properties strongly change—there is a high divergence in the electrical properties. This is explained with the formation of a network system of the fillers and by the decrease of the correlation length ($\xi \sim |p - p_c|^{-v}$) for increasing mass fraction of the fillers as stated by percolation theory [12]. The correlation length is the average distance of two sites belonging to the same cluster, and the percolation exponent v has the value ~0.88 for 3D percolation. Most physical quantities diverge at the percolation threshold and this divergence can be related to the correlation length. For instance, the conductivity (Σ) of random mixtures of superconducting (fraction p) and normal-conducting $(1-p)$ elements, near the percolation threshold, has a power law dependence ($\Sigma \sim |p - p_c|^{-s}$). The exponent s also appears in the critical behaviour of the dielectric constant in random systems [13]; it is called the superconducting exponent and has the value of 0.75 ± 0.04 [14] for the 3D case.

In this way, the composite dielectric constant near the percolation threshold can be predicted by the following power law [15].

$$\varepsilon_{\text{eff}} = \varepsilon_{\text{matrix}}(f_c - f)^{-s}, \qquad f \leqslant f_c. \tag{1}$$

Several numerical models have been developed for studying the effect of adding conductive fillers to a lossless dielectric matrix on the composite dielectric constant and dielectric strength. They can be divided into lattice-based models [16–21] and continuum models [22, 23]. The present

work is related to the continuum models where the conductive fillers are MWCNT.

　　The model developed by Gyure and Beale [22] approximates random conductor shapes to perfect conductor 2D cylinders. The cylinders are generated by the Monte Carlo method and the sample is placed in a square box where a potential drop between two sides of the box is applied. These two sides are modelled as capacitor plates that extend to twice the size of the sample. They then apply the boundary element method to find the approximate solution for each conductor. Knowing the potential in each conductor, they determine the potential drop between two conductors and compare that to the dielectric strength of the material. This is done by dividing the potential drop between two conductors by the minimal surface separation distance. The simulation is started with a potential drop equal to the length of the sample producing a uniform field **E** normalized to 1. They assume that the local breakdown occurs in the sample, where the electric field is maximum ($\mathbf{E}_{max}$). The maximum electric field is stored at each iteration. Once the breakdown occurs, the constraints in the equations are updated and solved iteratively until the formation of at least one conductive path which discharges the capacitor. The breakdown field is defined as the inverse of the minimum $\mathbf{E}_{max}$. The breakdown field, breakdown path geometry, and dielectric constant as functions of the metal-packing function are determined. Another model [23] was proposed to study the breakdown dynamics in uniform fields. The dielectric strength is calculated using the multipole expansions for 3D and 2D, allowing a faster calculation of the dielectric strength of the sample but a weaker definition of the conductive path or breakdown.

4. Model

The present model represents an extension of the capacitor plate model [22]. The charge density of the filler is approximated by cylinders, which is appropriate for cylindrical fillers such as multiwall carbon nanotubes (MWCNT).

　　This approximation has been validated for single wall nanotubes [24], and compared to the density functional theory it reveals an excellent agreement in the charge distribution. For the N-body problem the charge distribution can be formulated as a simple capacitance extraction problem. It can be solved using graph theory [25–27], which is a mathematical abstraction and an efficient method for analysing paths and networks. It has been widely employed to study electric conduction and even minimum travel distance problems, among others.

　　Results from the application of graph theory are interpreted in terms of possible paths for electrical conduction. This approach considers the distance between neighbouring conductors as well as their relative positions. The developed methodology can be applied both to carbon nanotubes and carbon nanofibres, with adjustments to the model parameters such as scale, shape and aspect ratio, etc.

　　In order to better understand the model description, some common definitions in graph theory are presented. The set of all vertices—v_i—is **V(G)** and the set of all edges—$e_k =$

$\{v_i, v_j\}$—is **E(G)**. A *directed graph* (**G**) is a finite collection of vertices together with directed edges (e_k) joining certain pairs of vertices with $\mathbf{G} = (\mathbf{V}, \mathbf{E})$. An *undirected graph* (**G**) is a finite collection of vertices $\{v_1, v_2, \ldots, v_n\}$ together with undirected *edges* $e_k = \{v_i, v_j\} = \{v_j, v_i\}$ joining certain pairs of vertices with $\mathbf{G} = (\mathbf{V}, \mathbf{E})$. A *path* (**P**) between vertices is a sequence of edges (with no repeated vertices) that allows one to proceed in a continuous manner from one vertex to another. The *length* of a path is its number of edges. A *cycle* (**C**) is a closed path (**P**), i.e., a path where the initial vertex (v_0) is equal to the final vertex (v_n). The *degree* (**k**) of a vertex (**k** (**v**)) in an undirected graph is the number of edges incident to (**v**).

　　The *incidence matrix* of a directed graph $\mathbf{G} = (\mathbf{V}, \mathbf{E})$ is a $|V| \times |E|$ matrix $A = a_{ij}$ such that

$$a_{ij} = \begin{cases} -1, & \text{if edge } j \text{ leaves vertex } i \\ 1, & \text{if edge } j \text{ enters vertex } i \\ 0, & \text{otherwise.} \end{cases} \quad (2)$$

　　The *average degree* of a graph ($\langle \mathbf{k} \rangle$) is the sum of all degrees (k_i) divided by the maximum vertex. In a more formal way it can be given by equations (3), where a_{ij} belongs to an adjacency list [26].

$$\langle k \rangle = \frac{\sum_{i \in V(G)} \sum_{j \in E_i(G)} a_{ij}}{\max(V(G))}. \quad (3)$$

4.1. Model description

In our model the nanotubes are perfect conductors, and are randomly dispersed in an isotropic homogeneous dielectric matrix. A graph is built to represent the nanotube network. The graph edges represent the charge of a local capacitor, the nodes are the conductors (plates of the local capacitor), and the edges containing the virtual nodes—source (s) or sink (t)—represent a perfect conductor, (plates of an exterior capacitor). The local capacitors only have two states, charged and uncharged. The sink (t) and the source (s) are connected to a potential drop represented by an edge. The capacitance is found by solving a capacitance extraction problem for two cylinders [28–30] using the dielectric constant of the matrix. It is assumed that the only way for the capacitors to discharge is through dielectric breakdown. To simulate capacitor discharge, the voltage between the virtual nodes is continuously increased until a point is reached where the dielectric is not capable of sustaining any further voltage increase. This will result in the formation of a permanent conductive channel between the two conductors. In this way, the breakdown procedure is conducted locally. The dielectric breakdown occurs first in a pair of conductors; the global domain starts conducting when one (or more) path for conduction is created between the virtual nodes. Thus, by applying a potential drop from s to t in small steps, and looking for the local electric field strength between two conductors, it can be determined if a conduction path has been created. The composite dielectric constant is calculated using the capacitance of the exterior parallel plate capacitor in vacuum, a method similar to the experimental procedure. In the following subsection the algorithm that is used is specified.

4.2. Algorithm

(a) *The initial graph G and the minimum distance vector.* Using a minimum distance function and a cut-off radius, that is the maximum interaction distance between two conductors, an initial undirected graph can be constructed. In order to apply the Kirchhoff circuit laws, the initial graph needs to be connected between the two virtual vertices. By applying the deep-first search algorithm [26] it can be found whether the initial graph is connected. If it is connected, then there is a subgraph which includes two exterior vertices *s* and *t*, with these two exterior vertices being a virtual representation of the exterior potential drop. Removing from the initial adjacency list the vertices that are not contained in the subgraph, it can be said that the graph is connected and the updated adjacency list represents this graph.

(b) *The capacitance vector.* In the previous step a connected graph is built. Now the Kirchoff circuit laws can be applied to solve the problem by the formulation of a capacitance extraction problem [28–30]. This problem is then solved for each edge in the adjacency list stored in the vector $C_{|E|}$. Knowing the capacitance in each edge, we can build a virtual electric circuit where the edges represent the capacitors and the vertices the plates of the capacitor.

(c) *The incidence matrix A.* In this step the incidence matrix from the initial graph is constructed. The edge directions are assigned from the higher vertex number to the lower vertex number.

(d) *Adding the voltage edge between s and t.* This ensures that theorem 2.2.1 [27], for the unique solvability of the network, is obeyed.

(e) *Finding the null space matrix (N) of A.* The null space is obtained from the integer matrix *A* in the reduced row echelon form. The retrieved null vectors represent the Kirchhoff voltage laws.

(f) *Form the **b** vector.* The **b** vector represents the charge conservation law. In the last row of the vector the external applied potential is added. This implies the removal of the last edge in the null vectors matrix.

$$\mathbf{b} = \left[\frac{0}{-v} \right],$$

where v is the exterior applied potential drop.

(g) *Form the Kirchhoff voltage law matrix.*

$$K_{VL} = N_{nx|E|}^{\mathrm{T}} \left(I_{|E|} C_{|E|}^{-1} \right)$$

where n is the number of null vectors and I the identity matrix.

(h) *Solving using the singular value decomposition the over determined linear system.*

$$\left[\frac{A}{K_{VL}} \right]_{(n+|V|)x|E|} [Q_E]_{|E|} = \mathbf{b}.$$

(i) *Testing for each edge in the graph if the maximum electric field is larger than the dielectric strength.* The capacitor equation is solved in order to obtain the potential drop in
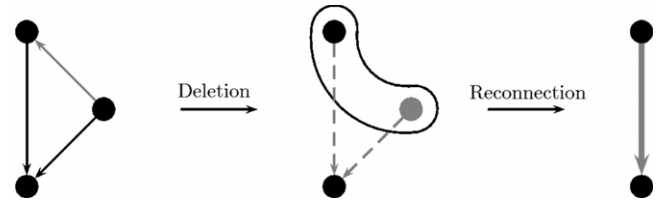

Figure 1. Illustration of the edge deletion process. The first grey edge is deleted, the capacitances on the dashed grey edges are added, and the grey node is removed.

each edge. Then, this value is divided by the minimum distance between two conductors, which gives a good approximation on the maximum electric field ($E_{\max}$). As a final step, this maximum electric field is compared to the dielectric strength.

(j) *If step (i) is true, the edges are removed and added to G′.* Removing an edge in the graph, means removing the capacitors with an electric field larger than the dielectric strength and replacing them by a thin conductor with no resistance in the circuit. The removed edges are added to a new graph with the same number of vertices (initially unconnected) G′. The value of $E_{\max}$ is stored at each iteration. This is necessary since our definition of breakdown field is the same as in [22, 23]; that is, as the inverse of the minimum $\mathbf{E}_{\max}$ normalized with respect to the breakdown field of the background dielectric.

Removing an edge is not a simple procedure. It implies the reconnection of all the incident edges and the removal of one vertex, as the two conductors are transformed into one by the thin conductor. Thus, one vertex is removed and the other vertex represents the new conductor with an increased surface area. The capacitance in all the edges that include the vertex representative of the new conductor also changes. The recalculation of the capacitance is not needed; it is just necessary to add the capacitance of the edges that are in parallel. In figure 1 we demonstrate this.

(k) *Test if s and t in graph G′ are connected.* The G′ graph is used to calculate the paths of conduction by using the Deep-First Search algorithm to test if the graph is connected. When this happens, the iteration stops, otherwise, a new incidence matrix is constructed without the removed edges.

(l) *Iterate from (d) until G′ is connected.*

5. Simulation procedure

In the first step of the simulation, materials were generated on the computer to represent the nanocomposites of interest to this study. The nanotube network is created first, using a simple derivation of the sequential packing algorithm proposed in [31]; see figure 2. The algorithm can be employed for several types of geometric objects. For instance, an extension of the same algorithm was used to study the random packing of grains with arbitrary shape [32].

All the results presented pertain to 50 cylinders with an aspect ratio of 10 (14 nm radius and 140 nm length) and
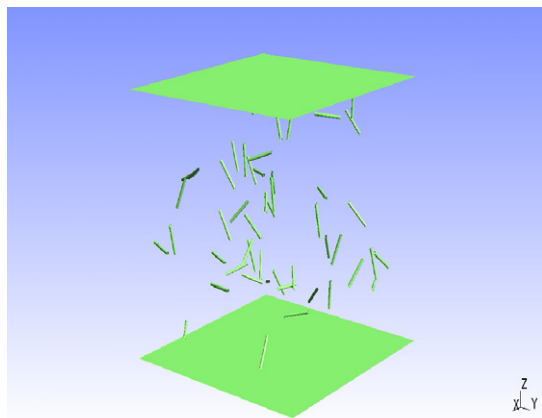
Figure 2. Random nanotube network. The area of the plates is much larger than the distance between them. For visualization purposes, only a part of the plates was represented in this figure. The length of the side of each plate is at least two times larger than the distance between them.

for each concentration we average ten different materials. The selected aspect ratio was the most suitable in relation to the experimental values. In general, increasing the cylinder aspect ratio will decrease the critical volume fraction [10] and increase the charge stored in the composite; this was studied in a previous work with an early version of the software [33].

We also use a constant average degree (50.9) to take into account the long range of the Columbic potential, that is, all cylinders are interacting with each other. Experimental values of 7.0 for the α-PVDF dielectric constant and 2.0×10^8 V m^{-1} for the dielectric strength were used.

The relatively low number of cylinders is not critical, as we are not using a stochastic model. Simulations performed with lower and higher number of cylinders for the same concentrations (by changing the simulation cell volume) show identical results, but with lower standard deviation.

A minimum separation threshold of 1.0 nm was also defined with the purpose of not taking into account quantum tunnelling effects. The value for this threshold is based on predictions of the order of the tunnelling distance as 10 Å [34].

6. Results and discussion

6.1. Effects of the nanofibre network arrangement on the capacitance

The effects of the relative orientation of the nanotubes and the distance between them on the capacitance are some of the key parameters defining the final macroscopic response of the nanocomposites.

For the study of the effect of the distance between the nanotubes, initially the cylinders are placed parallel to each other, with an axial orientation along the *y* axis. In a first study (represented in figure 3(a)), one cylinder is fixed and the second is translated along the *y* axis in small steps. At each step, the capacitance extraction problem is solved. The results of this study are represented in figure 5(a) as *translation y*. In a second study, the initial position of the cylinders is equal to

the one described for the previous study, but now one cylinder is fixed and the second one is translated along the *x* axis (represented in figure 3(b)). The results of this study are represented in figure 5(a) as *translation x*.

For the study of the effect of the relative angle between nanotubes, the cylinders are initially placed parallel to each other, with an axial orientation along the *y* axis. Then, the capacitance is calculated whilst maintaining the first cylinder fixed and rotating the other cylinder about the *x* axis (represented in figure 4(a)), or about the *z* axis (represented in figure 4(b)). The results of this study are shown in figure 5(b).

Figure 5 shows the capacitance variation for a pair of cylinders when the relative orientations and distance are changed. As could be expected, the capacitance decreases with the distance between fibres. In the case of an increase in distance when a cylinder is displaced along its main axis (translation along *y*), there is a slower decrease of capacitance with distance. This fact is related to the size of the contact surface area, which is decreasing linearly when the two cylinders are displaced relative to each other.

There is also a significant influence of the rotation of the cylinder about the *z* axis, since the distance between cylinders decreases considerably, in fact up to half the original distance at rotation angles of 90° and 270° (even though the surface area that is at the minimum distance at these angles is much smaller than at 0° and 180°). However, the capacitance is not significantly affected by rotation about the *x* axis, even at a 90° rotation angle, implying that in practical terms, the distance has a much stronger effect than the rotation angle.

The value of the capacitance does not change considerably with the rotation around a plane parallel to the fixed cylinder. This occurs because even at large rotations of one cylinder about the *x* axis, only the centre region of the two cylinders is at the minimum distance between them, but the distance between any other points on the surface of the two cylinders is not significantly different.

6.2. Composite dielectric constant

In figure 6(a) are shown the experimental and simulation results of the dielectric constant for several concentrations. The simulated dielectric constant has a scaling difference of 1E6 relative to the experimental values. This is expected, as in the proposed algorithm only cylinder–cylinder capacitances are calculated, and it is assumed that inside the cylinder the dielectric constant is the same as the lossless matrix. It should be noted that since we impose a constant aspect ratio during the generation of the material, we do not consider the possibility of two or more nanotubes sticking together and altering the effective aspect ratio.

Because of these approximations, figure 6(b) shows the normalized simulation results using equations (4).

$$\varepsilon_n = \varepsilon_{\text{PVDF}} \left(\frac{\varepsilon - \varepsilon_{\min}}{\varepsilon_{\min}} + 1 \right). \tag{4}$$

The trends and values of the simulation are similar to the experimental ones. It can be observed that the critical concentrations are similar; in the simulation it is 0.0011 and
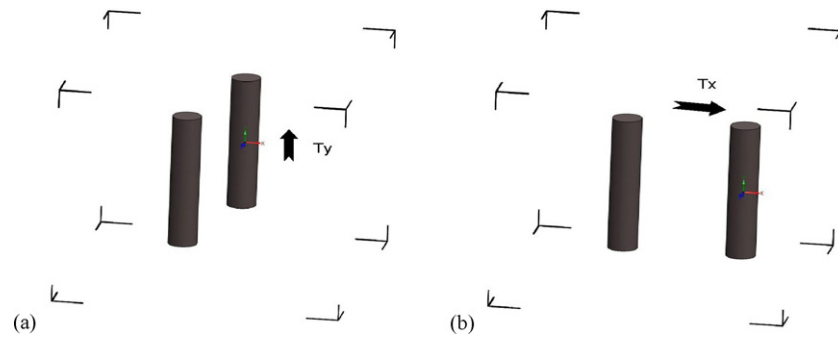
Figure 3. Representation of fibre translation along: (a) the *y* axis, and (b) the *x* axis.
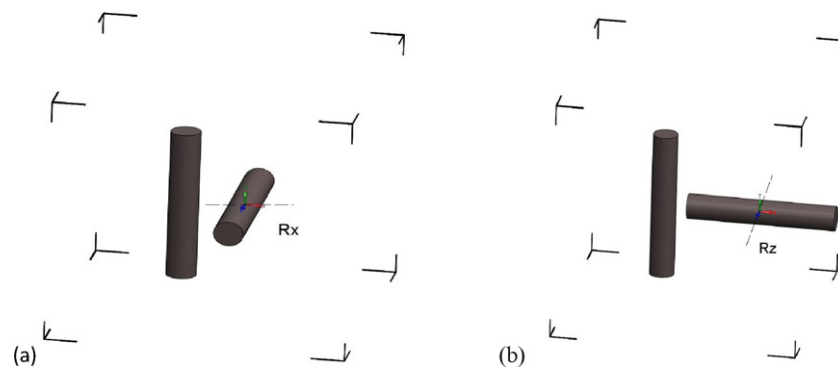

Figure 4. Representation of the relative rotation about: (a) the *x* axis, and (b) the *z* axis.
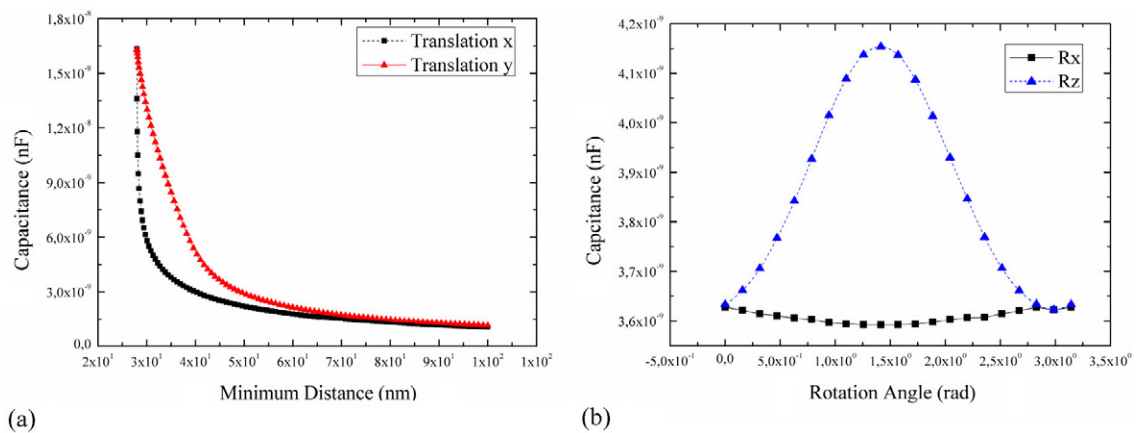

Figure 5. (a) Effect of the distance between two nanotubes on the capacitance. (b) Effect of the angle between two nanotubes on the capacitance.

in the experiments 0.0016 (2.0 wt%). These concentrations disagree with the MWCNT/PVDF composite study by Wang and Dang [7] (0.0161), and are more in agreement for the same type of composites with Ahmad [8], 0.0079. The best fit using a nonlinear least square algorithm in a log–log plot of the dielectric constant with equation (1) yields $s = 0.29 \pm 0.09$ for the simulation and $s = 0.22 \pm 0.09$ for the experimental values without normalization. Using the critical concentration from the experiments, the simulation results yield $s = 0.28 \pm 0.09$. These exponents and the corresponding errors are in the same interval, validating the assumption that highly dispersed MWCNT nanocomposites form capacitor networks.

Compared with MWCNT/PDVF exponents $s = 0.31$ [7] our data error interval includes the latter value, but disagrees with the universal value for the superconductivity exponent (0.75).

The fitting error is large, indicating that the available data is insufficient to determine the power law attributes (equations (1)). The dielectric constant is expected to increase with nanotube content when approaching the percolation threshold for small concentrations and decrease above the percolation threshold. The latter is in disagreement with our experimental and simulation results and with the percolation law. This type of behaviour has also been observed for composites of polycarbonate and either MWCNT or carbon
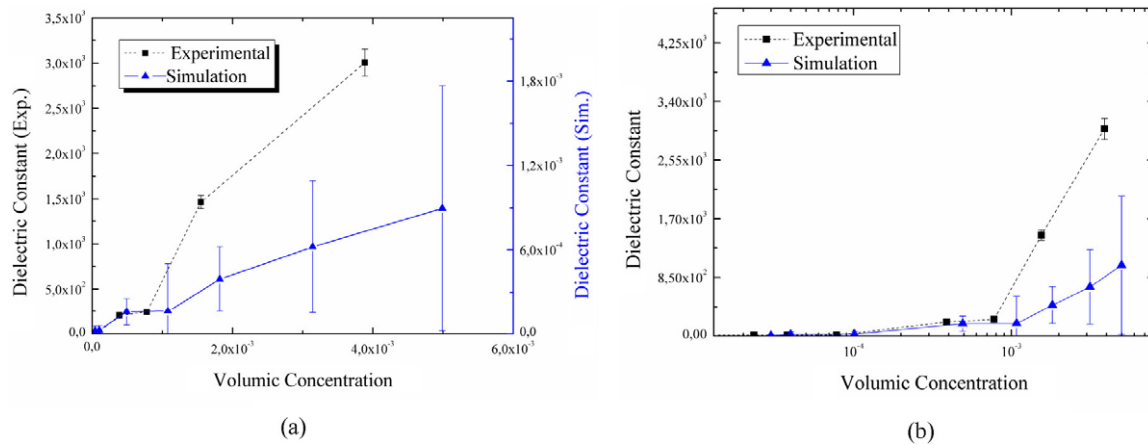
6

Figure 6. (a) Experimental and simulated dielectric constant versus nanotube volume concentration. (b) Experimental and normalized simulated dielectric constant.
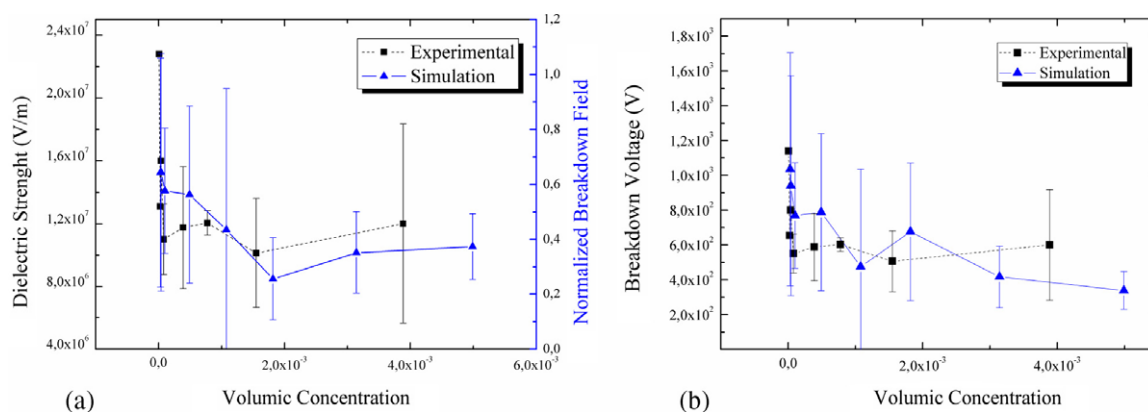

Figure 7. (a) Experimental dielectric strength and normalized breakdown field versus filler volume concentration. (b) Simulated breakdown voltage versus filler volume concentration.

black; as reported in [35] and references therein. This also records a low percolation concentration between 1.0 and 1.5 wt%. For the same type of composite (MWCNT/PC) a low percolation value (1.0–1.5 wt%) was also reported in [36]. These values agree with ours by noting that our MWCNT breaks during the fabrication process due to the high applied electrical field, lowering the aspect ratio as explained before.

The previous sections show that for low variations in the minimum tube–tube distance, below 45 nm in the initial separation, the capacitance has a higher increase for the same variations at distances larger than 45 nm. Thus, the critical concentration is related to the MWCNT orientation and minimum tube–tube distance. It should also be noted that, in the present simulation, contact between the nanotubes was not allowed. In this case, it is clear that the increase in the permittivity and the critical concentration is not related to formation of 'contact' networks, but simply with geometrical factors related to the capacitance. After the critical concentration, the simulation diverges relative to the experimental values. In this regime, the probability of contact between the MWCNT is very small or not possible [10] but we cannot state the same for the contact between MWCNT clusters. Similarly, in real situations, it is not possible to have

a single aspect ratio in the MWCNT but there is a distribution of aspect ratios.

Another important topic concerns the deviation bars found in figure 6; these are related to the effect of the minimum distance and the rotation angle as previously explained. For higher concentrations the deviation increases. As the separation between the MWCNT decreases, small changes in the distance result in a strong change in the tube–tube capacitance.

The high value of the critical concentration in [7], relative to those found in the present work, is high enough to indicate the formation of a 'contact' network [10]. This fact may explain the superb agreement between the experimental results of [7] and the percolation law. Also, based both on our results and on [35], it can be stated that for low values of the critical concentration, the percolation law is not accurate for describing the dielectric constant of the nanocomposite.

6.3. Composite dielectric strength

Figure 7(b) shows that the external voltage required to enable the formation of a conductive path decreases with the nanotube volume fraction. The error bars associated with the voltage calculation are also displayed and show

significant variations for small concentrations. This can be explained by noting that the orientation of each conductor influences the local capacitance of the composite; also, in the materials that were generated, small variations in the nanotube–nanotube minimum distances induces relatively large changes in breakdown. These two factors contribute to the large deviations of the overall values.

Figure 7(a) shows the normalized breakdown field using the experimental dielectric strength of the polymer, in the range of 2×10^8 V m^{-1}. The plot shows that the breakdown field decreases with concentration. Thus, the external breakdown voltage that is required for the formation of a conductive path decreases with the filler volume concentration. These results are in agreement with trends presented for spheres in [18, 19], through modelling and experimental testing. The last concentration in the numerical results cannot be obtained experimentally, as for these concentrations the nanocomposite is already conductive.

7. Conclusion

This work presents a numerical model, developed by the authors, which focuses on the effect of adding conductive nanotubes to the composite dielectric strength and in the dielectric constant. Simulation results are compared to experimental results on MWCT/PVDF nanocomposites. It is shown that below the critical concentration, highly dispersed conductive nanotubes form capacitor networks. It is demonstrated that the dielectric constant and the dielectric strength of the composite are highly dependent on the distribution of the nanotubes, resulting in high deviations of the electrical properties.

Finally, it is concluded that the percolation law is not the most accurate description at critical concentrations for this type of nanocomposite. Namely, from the percolation law, the dielectric constant is expected to increase with the filler content when approaching the percolation threshold for small concentrations and to decrease above the percolation threshold. Our experimental and simulation results indicate that anomalous percolative behaviour can be observed due to the formation of capacitor networks. The numerical results obtained thus confirm what had been suggested previously by several authors from experimental results for this type of nanocomposite.

Acknowledgments

References

[1] Landauer R 1978 *Electric Transport and Optical Properties of Inhomogeneous Media: AIP Conf. Proc.* ed J C Garland and D B Tanner (New York: AIP) No 4
[2] Chou T-W, Thostenson E T and Li C 2005 *Compos. Sci. Technol.* **65** 491
[3] Garnett J C M 1904 *Phil. Trans. R. Soc.* B **203** 385
[4] Bergman D J and Stroud D 1992 *Solid State Phys.* **46** 148
[5] Brosseau C, Quéfféléc P and Talbot P 2001 *J. Appl. Phys.* **89** 4532
[6] Cheng Y, Chen X, Wu K, Wu S, Chen Y and Meng Y 2008 *J. Appl. Phys.* **103** 34111
[7] Wang L and Dang Z-M 2005 *Appl. Phys. Lett.* **87** 042903
[8] Ahmad K and Pan W 2006 *Appl. Phys. Lett.* **89** 133122
[9] Zhu B-K, Xie S-H, Xu Z-K and Xu Y-Y 2006 *Comput. Sci. Technol.* **66** 548
[10] Munson-McGee S H 1991 *Phys. Rev.* B **43** 331
[11] Kuntman A and Kuntman H 2000 *Microelectron. J.* **31** 629
[12] Kirkpatrick S 1973 *Rev. Mod. Phys.* **45** 574
Stauffer D and Aharony A 1992 *Introduction to Percolation Theory* (London: Taylor and Francis)
[13] Wilkinsion D, Langer J S and Sen P N 1982 *Phys. Rev.* B **28** 1081
[14] Herrmann H J, Derrida B and Vannimenus J 1984 *Phys. Rev.* B **30** 4080
[15] Efros A L and Shklovskii B I 1976 *Phys. Status Solidi* b **76** 475
Bergman D J 1980 *Phys. Rev. Lett.* **44** 1285
Nan C W 1993 *Prog. Mater. Sci.* **37** 1
[16] Archangelis L, Redener S and Herrmann H J 1985 *J. Physique Lett.* **46** L585
[17] Duxbury P M, Beale P D and Leath P L 1986 *Phys. Rev. Lett.* **57** 1052
[18] Bowman D R and Stroud D 1989 *Phys. Rev.* B **40** 4641
[19] Gefen Y, Shih W H, Laibowitz R B and Viggiano J M 1986 *Phys. Rev. Lett.* **57** 3097
[20] Takayusu H 1985 *Phys. Rev. Lett.* **54** 1099
[21] Beale P and Duxbury P M 1988 *Phys. Rev.* B **37** 2785
[22] Gyure M F and Beale P D 1989 *Phys. Rev.* B **40** 9533
[23] Gyure M F and Beale P D 1992 *Phys. Rev.* B **46** 3736
[24] Li C and Chou T-W 2006 *Appl. Phys. Lett.* **89** 063103
[25] Bollobás B 1998 *Modern Graph Theory* (New York: Springer)
[26] Cormen T H, Leiserson C E, Rivest R L and Stein C 2001 *Introduction to Algorithms* 2nd edn (Cambridge: MIT Press)
[27] Recski A 1989 *Matroid Theory and its Applications in Electrical Network Theory and in Statics* (Berlin: Springer)
[28] Greengard L, Cheng H and Rokhlin V 1999 *J. Comput. Phys.* **155** 468
[29] Kim S, Nabors K and White J 1992 *IEEE Trans. Microw. Theory Tech.* **40** 1496
[30] Nabors K and White J 1991 *IEEE Trans. Comput. Aided Des. Integr. Circuits Syst.* **10** 1447
[31] Vold M J 1959 *J. Phys. Chem.* **63** 1608
[32] Coelho D, Thovert J F and Alder P M 1997 *Phys. Rev.* E **55** 1959
[33] Simões R, Silva J, Cadilhe A and Vaia R 2008 *Composite Interfaces* at press
[34] Balberg I 1987 *Phys. Rev. Lett.* **59** 1305
[35] Pötschke P, Dudkin S M and Alig I 2003 *Polymer* **44** 5023
[36] Pötschke P, Bhattacharyya A R and Janke A 2004 *Carbon* **42** 965